Identification of the role of autophagy-related TNFSF10/hsa-let-7a-5p axis in vitiligo development and potential herbs exploring based on a bioinformatics analysis

Wenwen Wang [a,b,2], Danfeng Xu [a,2], Youming Huang [a], Xiaohua Tao [a], Yibin Fan [a], Zhiming Li [b,**,1], Xiaoxia Ding [a,1,*]

[a] Center for Plastic & Reconstructive Surgery, Department of Dermatology, Zhejiang Provincial People's Hospital(Affiliated People's Hospital), Hangzhou Medical College, Hangzhou, Zhejiang, 310000, China
[b] Department of Dermatology and Venereology, The First Affiliated Hospital of Wenzhou Medical University, Wenzhou, Zhejiang, 325000, China

ARTICLE INFO

ABSTRACT

Background: Vitiligo is a common clinical disorder caused by the destruction of epidermal melanocytes, which is often associated with autoimmune mechanisms. Autophagy plays a crucial role in maintaining cellular homeostasis and exhibits close associations with various autoimmune disorders. While dysautophagy of melanocytes is associated with vitiligo pathogenesis, there is a lack of studies on autophagy-related genes (ARGs) in blood samples from individuals with vitiligo.

Methods: Blood samples from individuals with vitiligo and healthy controls were compared to identify differentially expressed genes (DEGs), which were subsequently subjected to further analysis. Then, miRNAs correlated with core genes were predicted by five distinct online tools, and those miRNAs that appeared in three or more tools at the same time were chosen for further enrichment analysis. Furthermore, *in vitro* experiments of targeting core genes were conducted.

Results: The results showed that there were a total of 30 ARGs among DEGs, with 13 up-regulated genes and 17 down-regulated genes. Based on the functional enrichment analysis of DEGs and projected miRNAs, we hypothesized that autophagy and apoptosis may synergistically contribute to the progression of vitiligo, with the TNFSF10/hsa-let-7a-5p axis potentially playing an important role that should not be ignored. In addition, epigallocatechin-3-gallate (EGCG) was found to be the common component in BAI GUO, CHA YE, and MEI ZHOU JIN LV MEI, which were discovered to be potential in vitiligo treatment by inducing cell autophagy and apoptosis targeting TNFSF10.

Conclusion: It was the first time that TNFSF/hsa-let-7a-5p was discovered to be involved in the development of vitiligo through autophagy and apoptosis. Meanwhile, we observed that BAI GUO, CHA YE, and MEI ZHOU JIN LV MEI were promising to treat vitiligo by regulating autophagy and apoptosis via TNFSF10. These findings could lead to new directions for investigating the pathogenesis and therapy of vitiligo.

* Corresponding author.
** Corresponding author.
  E-mail addresses: lzm7272@yeah.net (Z. Li), dingxiaoxia@hmc.edu.cn (X. Ding).
[1] These authors contributed equally to this work and should be considered as co-corresponding authors.
[2] These authors contributed equally to this work and should be considered as co-first authors.

1. Introduction

Vitiligo is a complex disease caused by the selective destruction of melanocytes, resulting in patchy loss of skin pigmentation [1]. The pathogenesis of melanocyte deficiency in vitiligo is multifaceted, in which autoimmune reaction playing a key role. However, there is currently a lack of specific treatment for vitiligo [2]. Previous studies have reported a high prevalence of autoimmune diseases among vitiligo patients, suggesting that studying blood transcriptomics could provide new insights into the disease [3,4].

A few pieces of evidence have recently emerged to support the role of autophagy in autoimmune diseases and other auto-inflammatory diseases, such as vitiligo [5], This suggested that autophagy may be an common mechanism involved in the development of vitiligo and other autoimmune diseases. Autophagy is an essential intracellular degradation system that plays a crucial role in maintaining cellular homeostasis and enhancing resistance against pathogen invasion [6]. Moreover, autophagy and apoptosis are two fundamental pathophysiological processes involved in regulating cells, exhibiting intricate interplay that profoundly influences the occurrence and progression of diverse diseases [7,8]. The analysis of autophagy-related genes (ARGs) in blood samples from vitiligo patients may offer novel insights into the pathogenesis and therapy of vitiligo. However, research surrounding the role of autophagy in vitiligo pathogenesis were focused on melanocyte cell lines and lesional areas of patients [9,10], as well as melanocytes and fibroblasts from non-lesional vitiligo skin [11], but not blood.

Microarray platforms are gradually gaining popularity as a method for identifying disease-related biomarkers and detecting genomic alterations [12]. Previous studies using microarray data have implicated several biomarkers and pathways in the development of vitiligo [13,14], but no research has focused on the autophagy-related biomarkers in the blood of vitiligo patients.

In this study, we used integrated bioinformatics methods to merge significant genes from two datasets, including blood samples from segmental vitiligo, non-segmental vitiligo, generalized vitiligo and healthy controls. The differentially expressed genes (DEGs) that overlapped with ARGs were used for hub gene discovery, enrichment analysis, interaction network creation, and pathway analysis. More importantly, we utilized online tools to predict the target miRNAs and then performed enrichment analysis of those miRNAs to identify potential therapeutic targets in the blood of individuals with vitiligo. Eventually, we discovered potential herbs that target core genes for the treatment of vitiligo. This study improved our understanding of the pathogenesis of vitiligo, especially the potential co-pathogenesis between vitiligo and other autoimmune diseases. Moreover, potential herbs for vitiligo treatment targeting ARGs were explored.

2. Materials and methods

2.1. Cell culture

The human melanocyte line PIG1 was purchased from ScienCell Research Laboratories, Inc (California, USA). The cells were cultured in Dulbecco's modified Eagle's medium (DMEM), which also contains 10 % fetal bovine serum (FBS) and 1 % streptomycin/penicillin.

2.2. Chemicals and regents

DMEM, FBS, and streptomycin/penicillin were purchased from Gibco (California, USA). Epigallocatechin-3-gallate (EGCG) and 3-Methyladenine (3-MA) were purchased from Sigma-Aldrich (Darmstadt, Germany). The CCK-8 assay kit was purchased from GlpBio (California, USA). HiScript® III All-in-one RT SuperMix Perfect for qPCR and Taq pro Universal SYBR qPCR Master Mix were purchased from Vazyme (Nanjing, China).

2.3. Dataset collection

Gene expression datasets were obtained from the Gene Expression Omnibus database (http://www.ncbi.nlm.nih.gov/geo), a public functional genomics database with high throughput gene expression sequencing data and microarrays data [15,16]. ARGs were acquired from the Human Autophagy Database (http://www.autophagy.lu/index.html), an autophagy-dedicated database that provides information on human genes involved in autophagy [17,18]. Immune-related genes (IRGs) were downloaded from the ImmPort database (https://immport.niaid.nih.gov), an open repository of participant-level large-scale human immunology data [19,20].

2.4. Data processing and differential expression analysis

The GSE dataset was used to download the normalised expression matrix of the microarray data. The annotation files from the dataset were then utilized for probe annotation. Next, the "limma R″ package was applied to identify DEGs in the dataset [21] (| Log2FC| > 1, p < 0.05), and a Venn plot was drawn between DEGs, ARGs and IRGs. Moreover, heatmap and box plot were conducted using the "heatmap" and "ggplot2" packages of R software. Spearman's correlation analysis was employed to analyze autophagy-related DEGs [22].

2.5. Functional correlation analysis

The "clusterProfiler" package was used to perform Gene Ontology (GO) analysis on DEGs [23,24]. GO is a standardized vocabulary for annotating gene functions [25,26]. GAGE was used to perform Kyoto Encyclopedia of Genes and Genomes (KEGG, http://www.genome.jp/kegg) pathway analyses [27], followed by visualization using the ggplot2 R package. The KEGG database integrates genomic and functional information, providing the gene and pathway annotations [28,29]. Significant enrichment was defined as false discovery rate (FDR) < 0.25 and $p < 0.05$ were considered significant enrichment. Engaged genes were red-labeled using the KEGG mapper.

2.6. Construction of the protein-protein interaction (PPI) network

To characterize the crucial DEGs, we used the online tool STRING (https://string-db.org/) to construct PPI networks with a minimum required interaction score of 4 [30]. STRING is a PPI network database based on public databases and literature information [31]. For further analysis, Cytoscape software was used to download interaction information. Significant genes were identified as hub genes using the cytoHubba plugin [32,33].

2.7. Functional insights of TNFSF10

GeneMANIA (http://www.genemania.org/) is an online platform that can predict the function of a gene or gene lists, as well as identify the physical interaction, genetic interaction, co-expression, pathway, co-localization, and shared protein domain [34,35]. Initially, we accessed the GeneMANIA database to acquire an interaction network of related connected genes for TNFSF10. The screening parameters were set as follows: Organism: Homo sapiens; Query Gene: TNFSF10; Maximum Resultant Gene: 20; Maximum Resultant Attributes: 10; Query-Dependent Weighting: Automatically selected weighting method. Then, the enrichment analysis of those genes was performed. Analyzing the sensitivity and specificity of TNFSF10 in vitiligo using the receiver operating characteristic (ROC) curve. To quantify the ROC, the area under the ROC curve (AUC) was calculated [36].

2.8. miRNA-mRNA network construction and functional insights of correlated miRNAs

The miRNA target predicting algorithms miRDB (http://mirdb.org/miRDB/) [37], TargetScan [38] (http://www.targetscan.org/), miRTarbase [39] (http://mirtarbase.cuhk.edu.cn/), ENCORI (https://starbase.sysu.edu.cn/) [40] and Diana-Tarbase V8.0 [41] (https://dianalab.e-ce.uth.gr/) were used to predict miRNAs targeting core genes. Only miRNAs predicted in 3 or more databases were used for subsequent network construction. Then, the interactions between those miRNAs and the differentially expressed mRNAs were obtained from DIANA-Tarbase and ENCORI. Cytoscape 3.6.0 software was used to visualize the target network, and the top 10 high-degree nodes were obtained using the cytoHubba plugin. An online tool, miEAA (https://ccb-compute2.cs.uni-saarland.de/mieaa2/), was used to perform the enrichment analysis of miRNAs [42].

2.9. Acquisition of Chinese herbs targeting core genes and vitiligo

HERB is a high-throughput experiment- and reference-guided database of traditional Chinese medicine (http://herb.ac.cn), which contains comprehensive information on Chinese herbs and their ingredients [43]. Firstly, we searched in the 'Disease' section of the website with 'vitiligo', while core genes were searched as the keyword in the 'Target' section. All correlated herbs were downloaded, and the overlapped herbs as well as the overlapped ingredients of those herbs were shown in Venn plots.

2.10. Cell viability assay

Using the CCK-8 test kit, cell viability was determined in accordance with the manufacturer's instructions. Briefly, PIG1 were seeded into 96-well plates at an initial density of 5000 cells/well and incubated in an incubator at 37 °C for 24 h. Subsequently, the cells were incubated with serum-free DMEM for 12 h and then treated with fresh medium containing different concentrations of 3-MA for 24 h. After cell treatment, 10 μL of kit reagent was added into 100 μL cell solution and incubated for further 90 min at 37 °C. Absorbance at 450 nm was measured with an enzyme-labeler and cell survival was calculated.

After that, The PIG1 cells were divided into control group, 3-MA group and 3-MA + EGCG group for another CCK-8 test. The medium without 3-MA and EGCG was selected as the control. The other two groups were starved for 12 h in serum-free DMEM, then treated for 24 h with medium containing 10 mM 3-MA, with or without 30 μM EGCG. Each sample was examined in triplicate, and each CCK-8 assay was repeated at least three times [44].

2.11. Quantitative real-time PCR

The total mRNA of the treated cells was isolated using Trizol and 1 μg RNA was used to synthesize cDNA using the HiScript® III All-in-one RT SuperMix Perfect for qPCR according to the manufacturer's protocol. Quantitative real-time PCR was conducted with the SYBR Premix Ex *Taq*II and the iQ5 PCR Detection System (Bio-Rad Laboratories, Hercules, Calif). The denaturing, annealing, and extension conditions of each PCR cycle were 95 °C for 30 s, 95 °C for 10 s, and 60 °C for 30 s, respectively. Real-Time PCR primer

sequences are listed in Table 3. The $2^{-\Delta\Delta Cq}$ method was used to quantify the expression levels of target genes, with GAPDH as the internal control. All primers were synthesized by Sangon Biotech (Shanghai, China). Each sample was examined in triplicate, and each quantitative real-time PCR experiment was repeated at least three times [45].

2.12. Statistical analysis

All data were analyzed using GraphPad Prism 7 and presented as mean ± standard deviation (SD). The statistical significance was calculated using the Student's *t*-test. $P < 0.05$ (*) was considered statistically significant.

3. Results

3.1. Data preprocessing

Two datasets (GSE80009 and GSE90880) were found after searching the Gene Expression Omnibus database with the inclusion criteria of (1) patients with vitiligo; (2) blood samples. Specifically, 12 samples (4 healthy controls, 4 segmental vitiligo, and 4 generalized vitiligo) from GSE80009 and 14 samples (6 healthy controls and 8 non-segmental vitiligo) from GSE90880. Moreover, three other datasets were used for validation: skin samples from patients with vitiligo from GSE75819, blood samples from patients with systemic lupus erythematosus (SLE) from GSE50772 and rheumatoid arthritis (RA) from GSE15573.

3.2. Differentially expressed ARGs in vitiligo

We identified DEGs between vitiligo patients and normal controls from the GSE80009 and GSE90880 datasets. DEGs were determined by setting the cutoff to FDR <0.05 and |log2 (FC)| ≥1. A total of 2389 DEGs were obtained from the GSE80009 dataset and 11 DEGs from the GSE90880 dataset. We then analyzed the overlapped DEGs between vitiligo-related genes, ARGs and IRGs. As shown
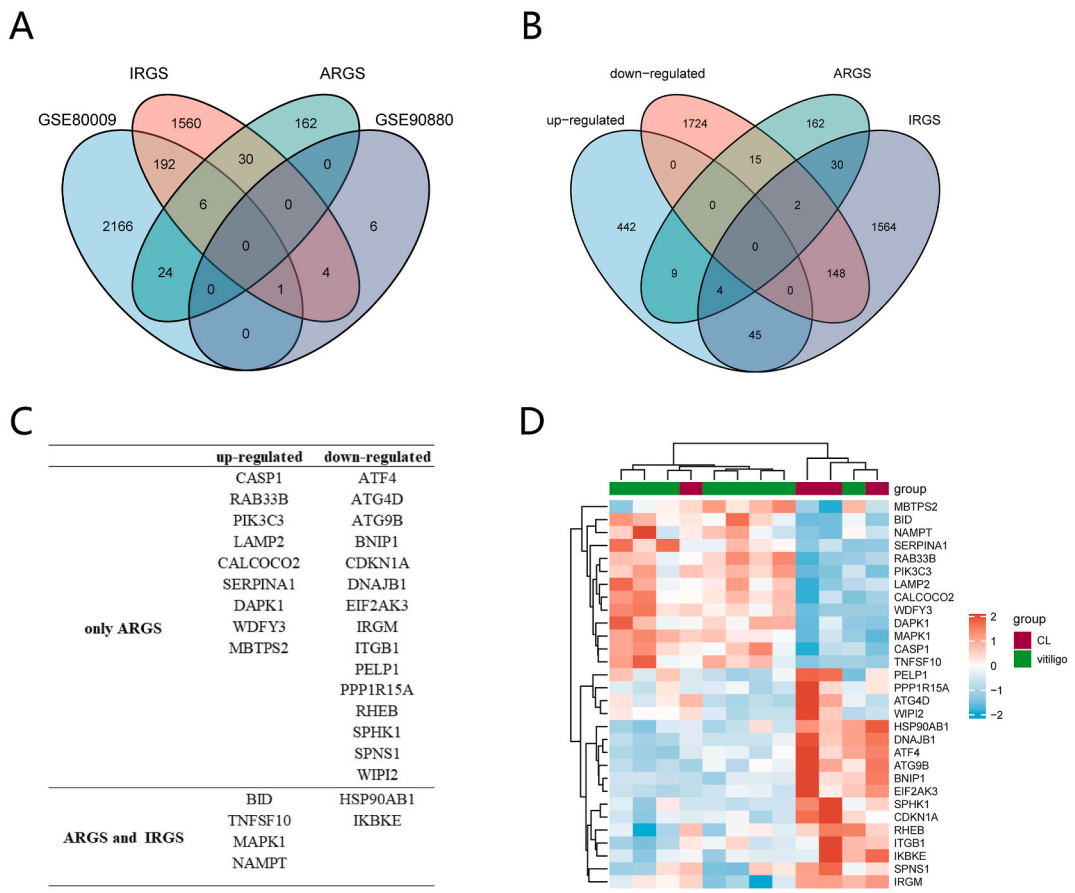

Fig. 1. Identification of DEGs. **(A–B)** Venn diagram was used to visualize common IRGs and ARGs shared between GEO datasets. **(C)** Information on the overlapping DEGs screened from the datasets. **(D)** Heat map visualization showing alternation for the 30 differentially expressed ARGs between vitiligo and normal groups.

in Fig. 1A, there were 30 ARGs among all DEGs from the two datasets, including 6 IRGs, all of which were from the GSE80009 dataset. Among them, 13 genes were up-regulated and 17 genes were down-regulated (Fig. 1B). The detail information of those genes was shown in Fig. 1C. After analyzing the GSE80009 dataset using R software, a heatmap was generated to present the differential expression of 30 ARGs between the vitiligo and normal groups (Fig. 1D). In addition, box plots were used to display the expression patterns of 30 ARGs that were differentially expressed between vitiligo and normal samples (Fig. 2A–C). There were 7 up-regulated genes (CASP1, RAB33B, TNFSF10, LAMP2, CALCOCO2, DAPK1, BID) and 9 down-regulated genes (SPHK1, WIPI2, SPNS1, ATG4D, RHEB, IKBKE, IRGM, DNAJB1 and HSP90AB1). Among them, TNFSF10, BID, HSP90AB1 and IKBKE were both autophagy-related and IRGs.

3.3. PPI network and correlation analysis of the differentially expressed ARGs

We performed PPI analysis to determine the interactions among differentially expressed ARGs. Fig. 3A illustrates the PPI network of these ARGs, while Fig. 3B displays the number of interactions for each gene. Fig. 3C presents the results of correlation analysis conducted to explore the expression correlation of these ARGs. According to the result of interaction number and expression pattern, 3 up-regulated genes (CALCOCO2, TNFSF10 and LAMP2) and 2 down-regulated genes (WIPI2 and HSP90AB1) were focused. Among them, only TNFSF10 and HSP90AB1 were also IRGs.

3.4. GO and KEGG enrichment analysis of autophagy-related DEGS

Using R software, we performed GO and KEGG enrichment analysis to analyze the underlying biological roles of these differentially expressed ARGs. Enrichment of various functions was initially demonstrated through GO enrichment analysis (Fig. 4A). Subsequently, GO and KEGG enrichment analysis elucidated the expression of associated genes in distinct functional enrichment sets (Fig. 4B and 5A), while also highlighting potentially associated genes in several functions exhibiting significant enrichment (Fig. 4C and 5B). The results demonstrated that the most significant GO enriched terms were involved in processes utilizing autophagic mechanism, autophagy, cellular response to external stimulus and macroautophagy (biological process); vacuolar membrane, autophagosome, autophagosome membrane and phagophore assembly site (cellular component); GTP binding, phosphatase binding, protein phosphatase binding and CARD domain binding (molecular function) (Fig. 4A–D). In KEGG enrichment analysis, the differentially expressed ARGs were mainly involved in the processes of autophagy, influenza A, protein processing in endoplasmic reticulum and apoptosis (Fig. 5A–C).

3.5. Validation of autophagy-related DEGS in vitiligo lesions

Vitiligo is characterized by depigmentation of the skin; therefore, we also conducted an analysis of the gene expression profile in ivitiligo-affected skin. There were 30 samples from 15 individuals' lesional and non-lesional skin of vitiligo patients in GSE75819. A total landscape of gene expression in GSE75819 was presented in a volcano plot (Fig. 6A), and the top 30 DEGs were shown in the heat map (Fig. 6B). Then, GO and KEGG enrichment analyses were performed to explore the potential biological functions of DEGs. The findings revealed that the most enriched GO keywords were nuclear part, nuclear lumen, intracellular non-membrane-bounded organelle, non-membrane-bounded organelle, nucleoplasm, RNA binding, microtubule cytoskeleton, mitotic cell cycle, mitotic cell cycle process and spindle (Fig. 6C). According to the KEGG enrichment study, DEGs played significant roles in Thermogenesis, Ribosome, Oxidative phosphorylation, Huntington disease, Parkinson disease, Spliceosome, RNA transport, Cell cycle, Nucleotide excision repair and Homologous recombination (Fig. 6D). Additionally, the vitiligo skin-derived DEGs were intersected with the vitiligo blood-derived DEGs, resulting in the identification of a single common gene, TNFSF10 (Fig. 6E).
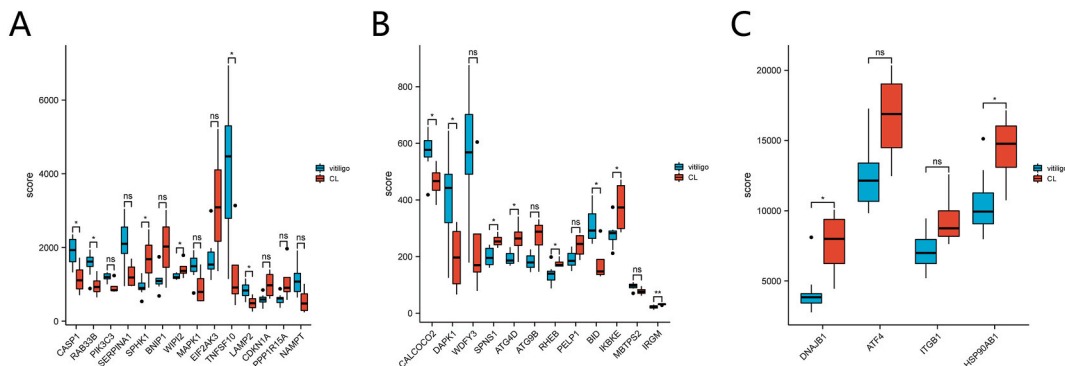

Fig. 2. The box plots of the 30 differentially expressed ARGs between vitiligo and normal samples.
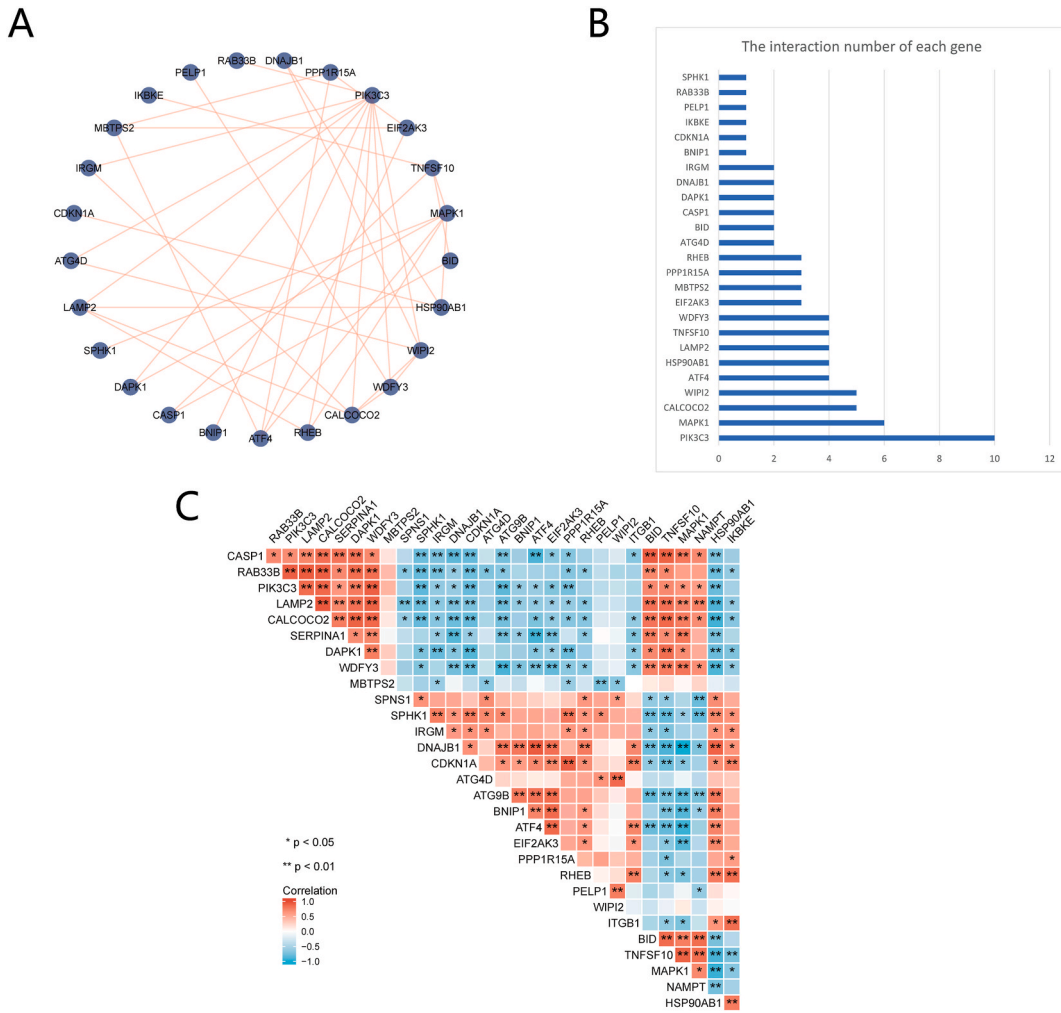
Fig. 3. Construction of the PPI network of the target genes to determine the interactions between differentially expressed ARGs. **(A)** The PPI network of target ARGs. **(B)** The interaction number of each gene. **(C)** The expression correlation of each gene.

3.6. Validation of autophagy-related DEGS in SLE and RA patients

Combined with the results of interactive score in PPI network and the expression patterns in vitiligo patients, we obtained one hub gene (TNFSF10). To verify the role of TNFSF10 in the pathogenesis of vitiligo and other autoimmune diseases, we analyzed the expression patterns of TNFSF10 in blood samples from patients with RA and SLE. As shown in Fig. 7A and 7B, we found that TNFSF10 was upregulated in both RA and SLE patients. Therefore, we speculated that TNFSF10 might be the crucial gene related to the overlapped pathogenesis of other autoimmune diseases that co-occur in vitiligo patients. To gain more detailed mechanistic knowledge about such cases, we conducted further analysis focusing on TNFSF10.

3.7. Functional insights of TNFSF10

We obtained 20 genes related to TNFSF10 from GeneMania (Fig. 8A), and then conducted GO and KEGG enrichment analyses. As shown in Fig. 8B and C, the significant GO enriched terms involved in apoptotic and tumor necrosis related processes. In KEGG enrichment analysis, the TNFSF10-related genes are mainly involved in the processes of apoptosis, necroptosis and TNF signaling pathway. Apoptosis was an overlapping pathway combined with the result of enrichment analysis of those 30 ARGs. Moreover, ROC analysis of TNFSF10 was performed in the vitiligo dataset, and it was found that the AUC value was 0.906 (Fig. 8D), which meant TNFSF10 also had a diagnostic value for vitiligo.
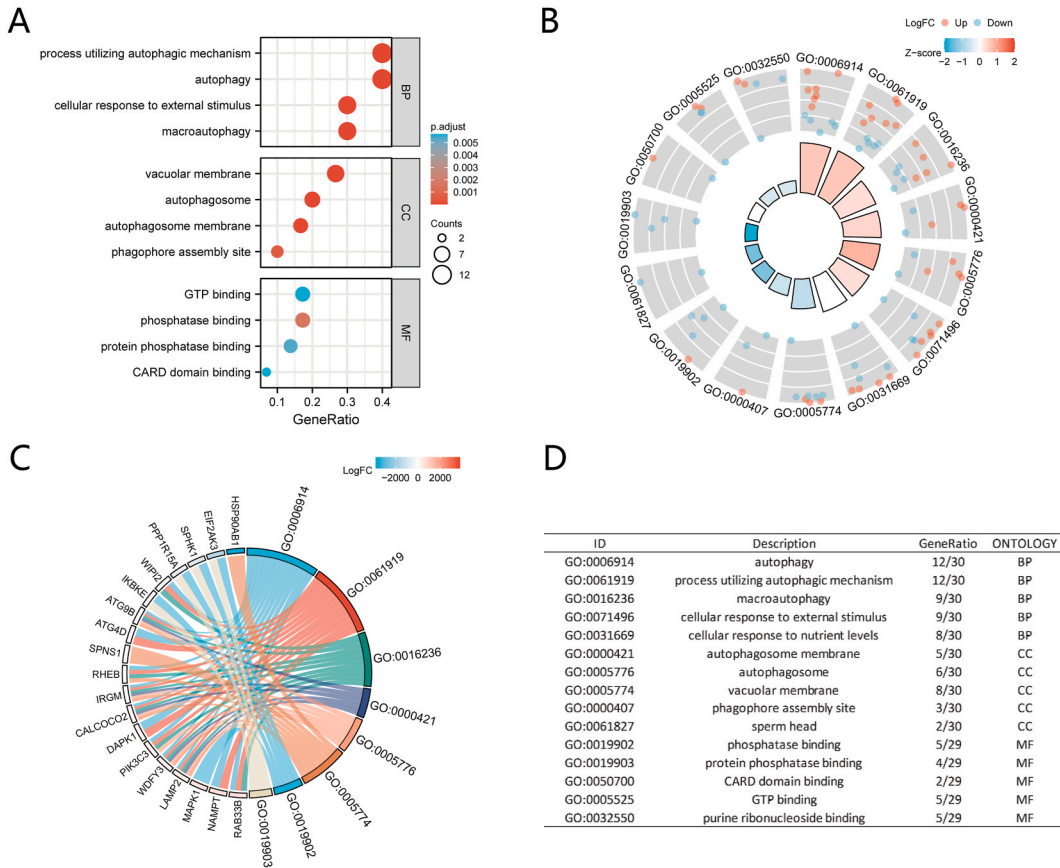
Fig. 4. Distribution of 30 ARGs for GO enrichment. **(A)** Bubble plot of enriched GO enrichment. **(B)** Circle plot of enriched GO enrichment. **(C)** Chordal graph of enriched GO enrichment. **(D)** The description of the GO labels. BP: The biological process; CC: cellular component; MF: molecular function.

3.8. miRNA-mRNA network construction

Firstly, as shown in Fig. 9A, a total of 13 miRNAs were eligible (in 3 and more databases at the same time). Then, the interaction between these miRNAs and 16 differentially expressed mRNAs was predicted using StarBase and Tarbase. As depicted in Fig. 9B, the network included 12 miRNA nodes and 11 mRNA nodes. The top 10 high-degree nodes were presented in Fig. 9C. Among them, 1 miRNA (hsa-let-7a-5p) and 2 mRNAs (LAMP2, TNFSF10) were found to have the highest interaction number count (Fig. 9D and E).

3.9. Functional insights of engaged miRNAs

The miRNAs involved in the network were analyzed for enrichment using an online tool called miEAA, which is accessible at https://ccb-compute2.cs.uni-saarland.de/mieaa2/. As shown in Table 1, almost all engaged miRNAs were involved in autophagy and apoptosis as well as the signaling pathways associated with both. These signaling pathways included mTOR, AMPK, p53, NF-kappa B signaling pathway and etc. Moreover, it was found that has-let-7a-5p was specifically found in blood (Table 2).

3.10. Potential herbs targeting core genes and vitiligo

Based on the above results, we speculated that autophagy and apoptosis might synergistically promote the development of vitiligo. TNFSF10, BID, MAPK1, ATF4 and EIF2AK3 were found to participate in apoptosis (Fig. 5B), while MAPK1, BID, IKBKE and CASP1 showed interaction with TNFSF10 in PPI network (Fig. 3A). Thus, TNFSF10, MAPK1 and BID were searched for herbs in 'Target' section. Besides, 'vitiligo', 'rheumatoid arthritis' and 'lupus erythematosus, systemic' were searched in 'Disease' section. As shown in Fig. 10A and 3 herbs (BAI GUO, CHA YE, MEI ZHOU JIN LV MEI) were explored targeting all targets. In addition, we found that those three herbs shared one common ingredient, called EGCG (Fig. 10B).
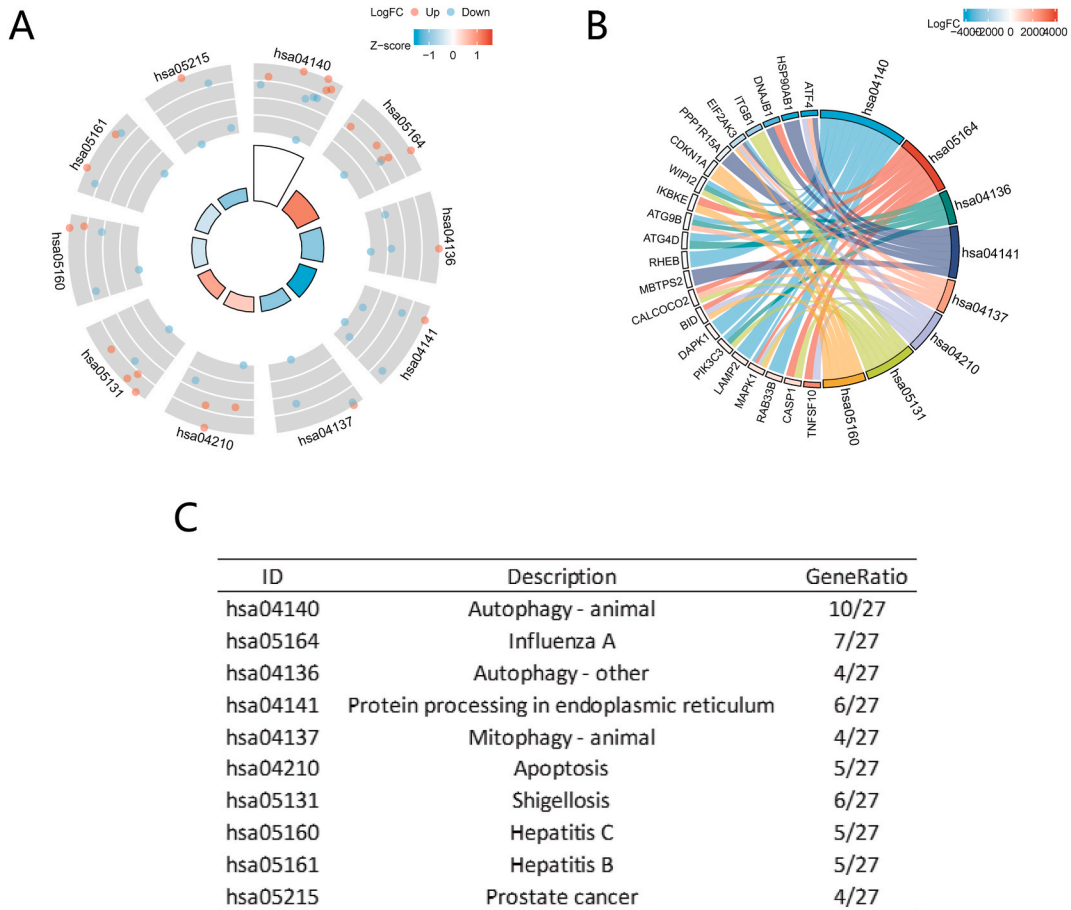
Fig. 5. Distribution of 30 ARGs for KEGG enrichment. **(A)** Circle plot of enriched KEGG enrichment. **(B)** Chordal graph of enriched KEGG enrichment. **(C)** The description of the KEGG labels.

3.11. EGCG decreases death in 3-MA-treated melanocytes

To verify this assumption, we treated PIG1 melanocytes with 3-MA and EGCG. We found that treatment with 3-MA decreased the viability and proliferation of PIG1 melanocytes (Fig. 11A). However, treatment with EGCG promoted the viability and proliferation of 3-MA-treated PIG1 melanocytes (Fig. 11B). To assess the involvement of TNFSF10, MAPK1 and BID in autophagy and apoptosis in vitiligo, we evaluated the relative expressions of these genes using real-time PCR. As shown in Fig. 11C, treatment with 3-MA induced the expression of TNFSF10, MAPK1 and BID, while EGCG inhibited this phenomenon.

4. Discussion

In this study, we focused on the expression patterns of ARGs in blood samples from vitiligo patients and conducted various analyses on those DEGs.

Firstly, mitophagy and ER processing were both revealed to be down-regulated according to the results of enrichment analysis of blood samples from vitiligo patients. According to prior research, defective ER-phagy and mitophagy were assumed to contribute to melanocyte destruction in vitiligo lesions under oxidative stress and an inflammatory microenvironment [46]. However, previous studies have primarily focused on the lesions of skin in vitiligo patients, such as Kyle J. Gellatly et al. who elucidated the intricate autoimmune network in vitiligo skin samples through scRNA-seq [47]. This study is the first to demonstrated that vitiligo blood also had deficient ER-phagy and mitophagy. Although our enrichment analysis of skin lesions from vitiligo patients did not reveal a direct correlation with autophagy, the GO keywords and KEGG pathways obtained through the analysis also exhibited certain associations with autophagy. For instance, studies have demonstrated that oxidative stress can induce cell death modes like apoptosis, autophagy, and ferroptosis in melanocytes, leading to immune responses and subsequent skin depigmentation [48]. Secondly, TNFSF10 was eventually discovered to be a critical autophagy-related gene linked to vitiligo and other autoimmune disorders. When the findings of enrichment analysis with TNFSF10 associated genes and 30 autophagy-related DEGs were combined, apoptosis was recognized as another overlapping pathway. As a result, we hypothesize that apoptosis and autophagy might work together to accelerate the
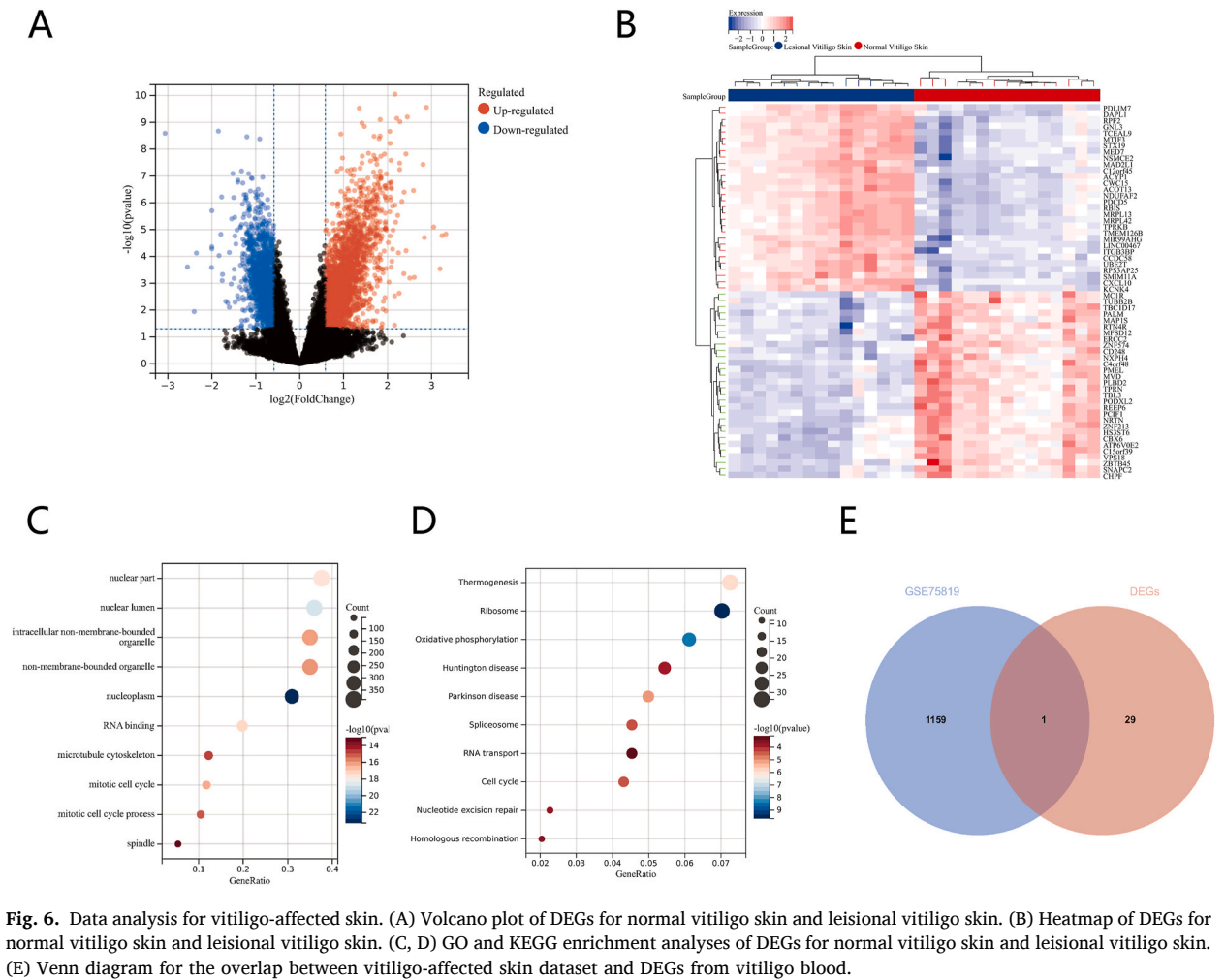
Fig. 6. Data analysis for vitiligo-affected skin. (A) Volcano plot of DEGs for normal vitiligo skin and leisional vitiligo skin. (B) Heatmap of DEGs for normal vitiligo skin and leisional vitiligo skin. (C, D) GO and KEGG enrichment analyses of DEGs for normal vitiligo skin and leisional vitiligo skin. (E) Venn diagram for the overlap between vitiligo-affected skin dataset and DEGs from vitiligo blood.
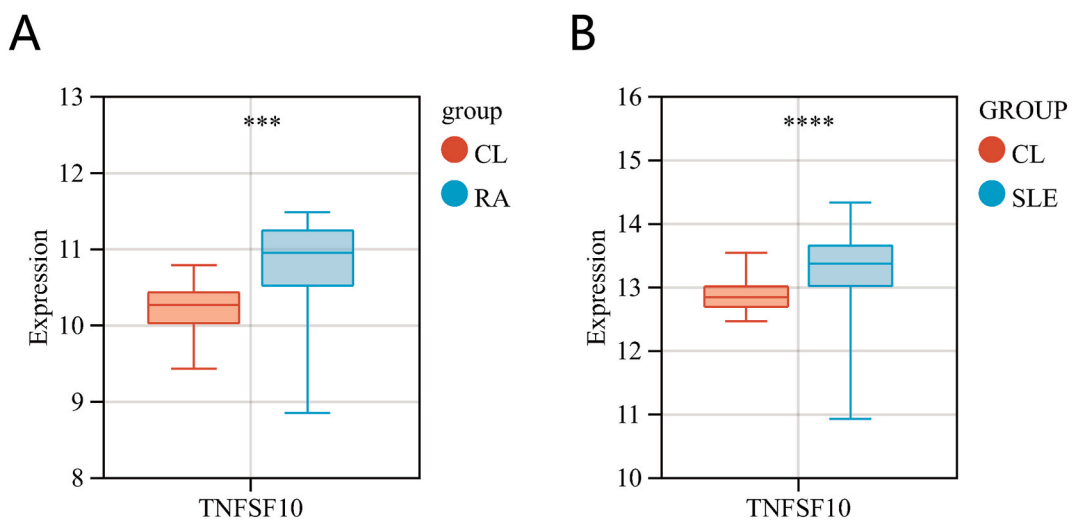

Fig. 7. The box plots show the expression level of TNFSF10 in blood samples of patients with RA**(A)** and SLE**(B)**.
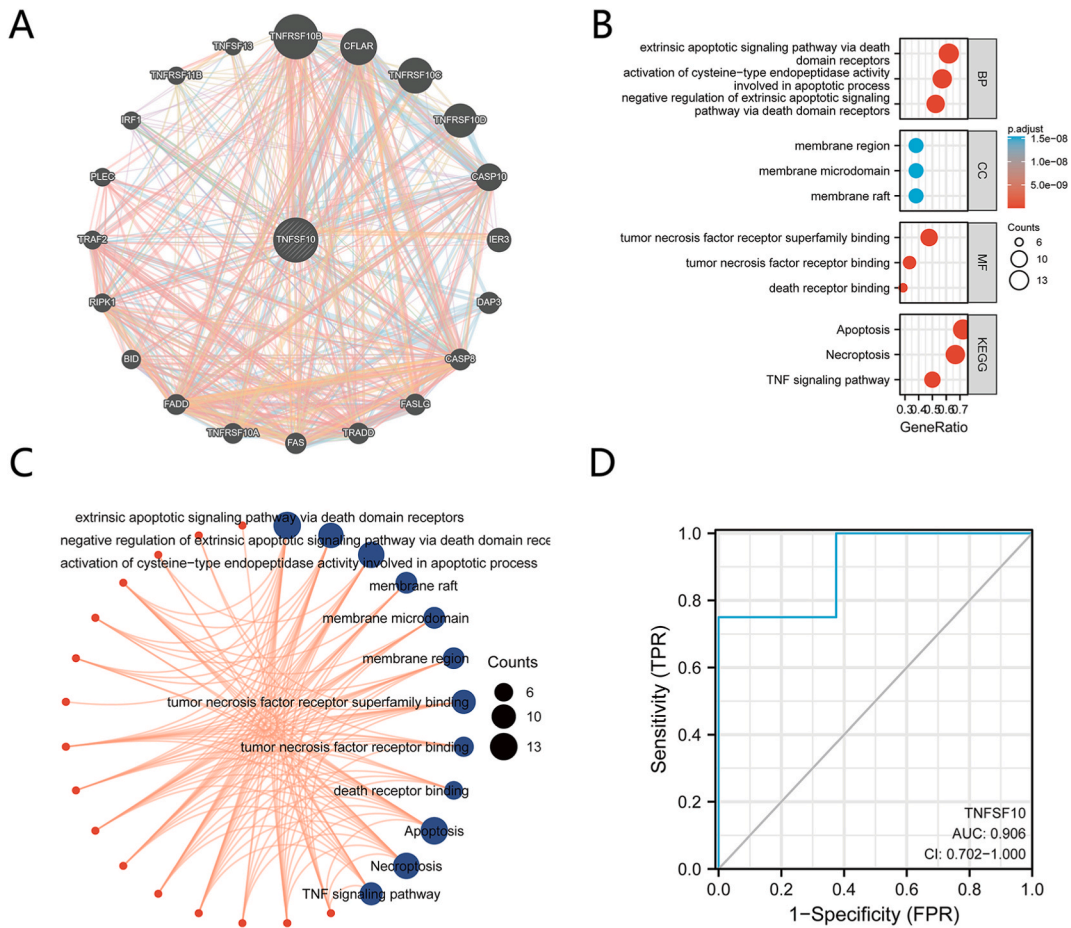
Fig. 8. Functional analysis of TNFSF10. **(A)** The related connected genes of TNFSF10 were analyzed using GeneMANIA. **(B–C)** Results of GO and KEGG enrichment Analysis of TNFSF10 related connected genes. **(D)** Results of ROC analysis of TNFSF10 in the vitiligo dataset.

development of vitiligo and perhaps other autoimmune diseases. The relationship between autophagy and apoptosis is intricate, as they collaborate in eliminating numerous cells, with autophagy also promoting apoptosis [49,50]. Similarly, the results of this study demonstrated that autophagy and apoptosis could synergistically contribute to the development of vitiligo through related genes, such as TNFSF10, BID and MAPK1. Apoptosis and autophagy might share common upstream signals [51], such as mTOR pathway and ROS [52,53]. We red-labeled 30 autophagy-related DEGs engaged in autophagy and apoptosis pathways (Supplementary Figs. 1 and 2), and we found that pieces of those autophagy-related DEGs also engaged in ER processing and MAPK pathway, which presented as common upstream signals of apoptosis and autophagy. TNFSF10, also known as 'Tumor Necrosis Factor-Related Apoptosis Inducing Ligand' (TRAIL, CD253), along with other closely related ligands (FasL, CD95L) [54], induces the signal transduction of apoptosis in tumor cells [55]. As reported, TNFSF10 is a promising anticancer agent for treating solid tumors, which has the unique property of inducing apoptosis in tumor cells while sparing normal ones [56–58]. It has also been reported that TNFSF10 was able to induce autophagy in certain cancer cells, however, how TNFSF10 induces autophagy has not been clearly elucidated [59]. MAPK8 activation mediated by TRAF2 and RIPK1 might be crucial for TNFSF10-induced autophagy [60]. Similarly, we found that TNFSF10 participated in both apoptosis and autophagy promoting the development of vitiligo.

In addition, we conducted enrichment analysis of predicted miRNAs in correlation with TNFSF10 and other 15 DEGs. The outcome revealed that most miRNAs are involved in apoptosis, autophagy, and correlated pathways such as the mTOR pathway, AMPK pathway, p53 pathway and so on. All these results suggested that the aforementioned miRNAs involved in the network had considerable credibility and might provide new insights into the potential cross-pathogenesis of vitiligo and other autoimmune diseases. Among them, hsa-let-7a-5p had the highest number of interactions and also exhibits blood specificity. The TNFSF10/hsa-let-7a-5p axis might offer novel insights into the pathogenesis and therapy of vitiligo. Moreover, we further explored the potential herbs that target autophagy and apoptosis for treating vitiligo. It was found that BAI GUO, CHA YE and MEI ZHOU JIN LV MEI meet the requirements, which shared a common ingredient called EGCG. While previous studies have utilized herbal medicines for treating vitiligo, this study delves deeper into elucidating its potential therapeutic mechanism [61].

Taken together, this study presented a novel approach by linking vitiligo and other autoimmune diseases with ARGs through blood analysis, which differed from the conventional studies on skin lesions. These findings suggested that an imbalance of autophagy and
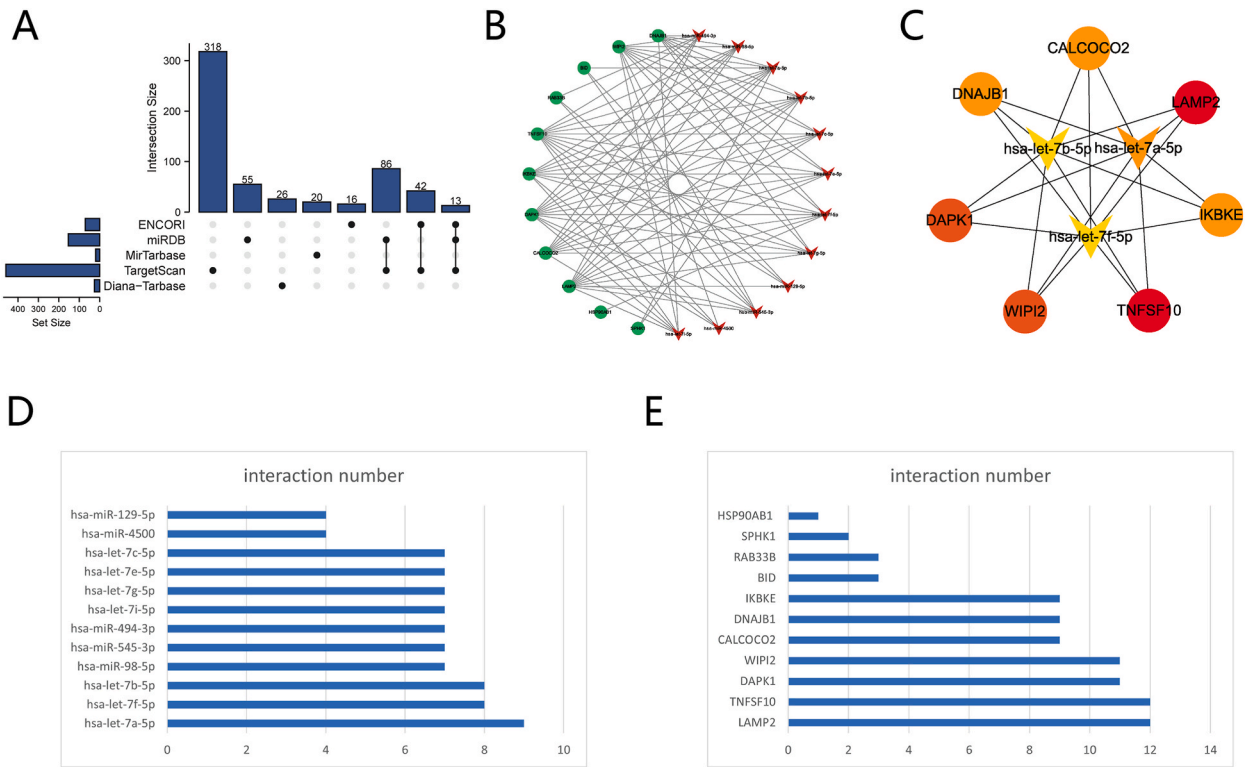
Fig. 9. The exploring and analysis of miRNAs. **(A)** Upset plot of overlapped predicted miRNAs targeting core genes using different online tools. **(B)** The miRNA-mRNA network. **(C)** The top 10 hub genes with the highest degrees of connectivity. **(D)** The interaction number of 12 miRNAs. **(E)** The interaction number of 11 differentially expressed mRNAs.

Table 1
Enrichment analysis of miRNAs in different signaling pathways.

Subcategory	Enrichment	P-value	Observed	miRNAs/precursors
Autophagy - animal	over-represented	0.009362	13	all
Autophagy - other	over-represented	1.90E-06	11	besides hsa-miR-670-3p; hsa-miR-494-3p
Apoptosis - multiple species	over-represented	6.34E-04	11	besides hsa-miR-670-3p; hsa-miR-545-3p
Necroptosis	over-represented	0.017446	12	besides hsa-miR-545-3p
lnfluenza A	over-represented	0.002959	13	all
NF-kappa B signaling pathway	over-represented	2.39E-04	13	all
TNF signaling pathway	over-represented	6.82E-04	13	all
p53 signaling pathway	over-represented	0.006088	13	all
mTOR signaling pathway	over-represented	0.01067	13	all
Protein processing in endoplasmic reticulum	over-represented	0.008512	13	all
lnsulin signaling pathway	over-represented	0.004056	13	all
Natural killer cell mediated cytotoxicity	over-represented	5.30E-04	13	all
Calcium signaling pathway	over-represented	0.015013	12	besides hsa-miR-545-3p
AMPK signaling pathway	over-represented	0.028354	12	besides hsa-miR-670-3p

apoptosis also existed in the blood of patients with vitiligo, and TNFSF10 might play an unignoring role in promoting the development of vitiligo through both apoptosis and autophagy. The TNFSF10/hsa-let-7a-5p axis might offer novel insight into the pathogenesis and treatment of vitiligo and other concomitant autoimmune diseases. In addition, Bai Guo, CHA YE and MEI ZHOU JIN LV MEI might be the promising herbs targeting autophagic and apoptotic pathways for the treatment of vitiligo. However, certain aspects of this study could be enhanced, such as the inclusion of a larger number of blood samples from vitiligo patients would obtain more scientific and convincing results. Furthermore, additional *in vitro* and *in vivo* experiments can be conducted in the future to reinforce the experimental evidence.

Table 2
Enrichment analysis of miRNAs in different organs.

category	subcatagory	Enrichment	P-value	miRNAs/precursors
Organs (miRWalk)	Lung	over-represented	2.66E-04	hsa-let-7b-5p; hsa-let-7e-5p; hsa-miR-98-5p; hsa-let-7i-5p; hsa-let-7a-5p; hsa-let-7c-5p; hsa-let-7f-5p; hsa-let-7g-5p
Organs (miRWalk)	Blood Platelets	over-represented	1.29E-06	hsa-let-7e-5p; hsa-miR-98-5p; hsa-let-7i-5p; hsa-let-7a-5p; hsa-let-7c-5p; hsa-let-7f-5p; hsa-let-7g-5p
Organs (miRWalk)	Fetal Blood	over-represented	5.81E-05	hsa-miR-129-5p; hsa-let-7e-5p; hsa-let-7i-5p; hsa-let-7a-5p; hsa-let-7c-5p; hsa-let-7g-5p
Organs (miRWalk)	Blood	over-represented	0.0036772	hsa-miR-129-5p; hsa-let-7e-5p; hsa-let-7i-5p; hsa-let-7a-5p; hsa-let-7c-5p; hsa-let-7g-5p
Organs (miRWalk)	Eukaryotic Cells	over-represented	1-17E-05	hsa-let-7e-5p; hsa-let-7i-5p; hsa-let-7a-5p; hsa-let-7c-5p; hsa-let-7g-5p
Organs (miRWalk)	Erythrocytes	over-represented	1.97E-05	hsa-let-7e-5p; hsa-let-7i-5p; hsa-let-7a-5p; hsa-let-7c-5p; hsa-let-7g-5p
Organs (miRWalk)	Megakaryocytes	over-represented	1.97E-05	hsa-let-7e-5p; hsa-miR-98-5p; hsa-let-7a-5p; hsa-let-7c-5p; hsa-let-7f-5p
Organs (miRWalk)	Erythroid Cells	over-represented	3.15E-05	hsa-let-7e-5p; hsa-let-7i-5p; hsa-let-7a-5p; hsa-let-7c-5p; hsa-let-7g-5p
Organs (miRWalk)	Plasma	over-represented	0.0022014	hsa-let-7e-5p; hsa-let-7i-5p; hsa-let-7a-5p; hsa-let-7c-5p; hsa-let-7g-5p
Organs (miRWalk)	Mucus	over-represented	5.80E-06	hsa-miR-98-5p; hsa-let-7i-5p; hsa-let-7f-5p; hsa-let-7g-5p

Table 3
Primers used for quantitative real time PCR assays.

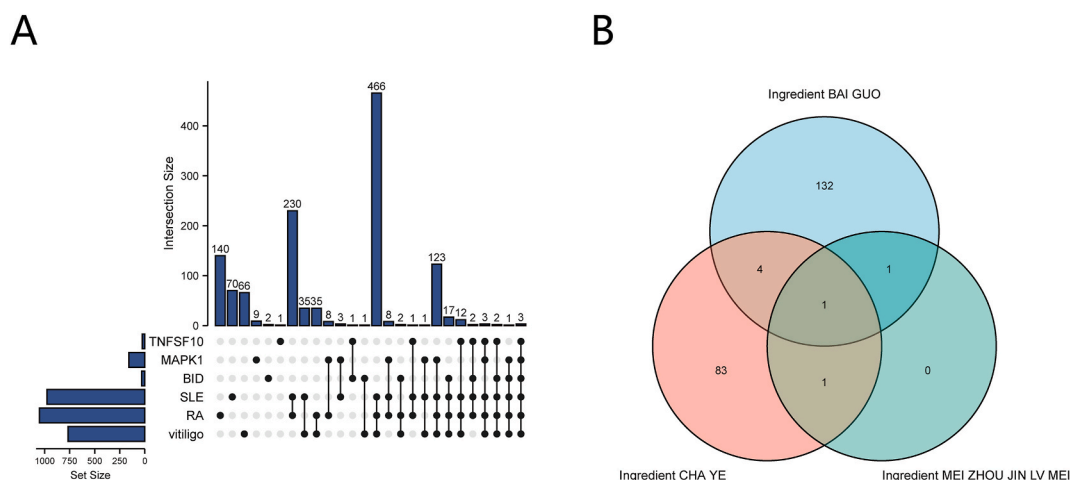| Gene	Direction	Primer sequence (5′ to 3′)
TNFSF10	Forward	GACCTGCGTGCTGATCGTGATC
	Reverse	GCTGACGGAGTTGCCACTTGAC
MAPK1	Forward	TCGCCGAAGCACCATTCAAGTTC
	Reverse	TCCTGGCTGGAATCTAGCAGTCTC
BID	Forward	GGCCTACCCTAGAGACATGGAGAAG
	Reverse	GCAAGGACGGCGTGTGACTG

Fig. 10. Screening of potential herbs. **(A)** Upset plot illustrating the predicted herbs. **(B)** Venn diagram showing the common components of BAI GUO, CHA YE, and MEI ZHOU JIN LV MEI.

5. Conclusion

In summary, our study had revealed the dysregulation of autophagy and apoptosis within the blood of vitiligo patients, and underscores the potential significance of the TNFSF10/hsa-let-7a-5p axis in regulating these processes. Additionally, Bai Guo, CHA YE and MEI ZHOU JIN LV MEI, which contain the common ingredient EGCG, exhibit promise as treatments for vitiligo. Our study presents a novel perspective on potential therapeutic approaches for vitiligo, yet further investigations are warranted to elucidate the intricate roles of autophagy and apoptosis in the initiation and progression of vitiligo.
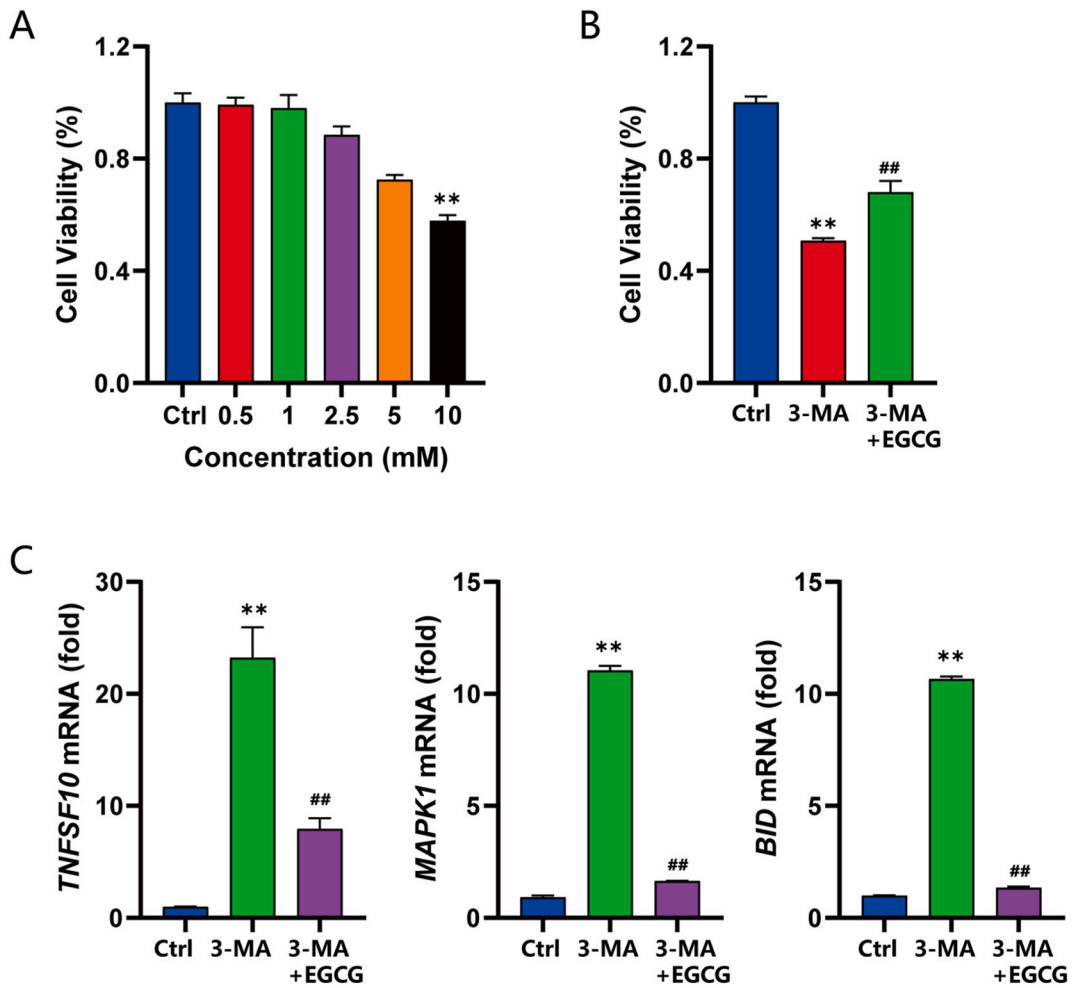
Fig. 11. Effects of EGCG on the 3-MA-treated PIG1 melanocytes. **(A)** The percentages of viable cells change in PIG1 after treatment with varying concentrations of 3-MA (0–10 mM). **(B)** The cell viability of PIG1 treated with 3-MA and 3-MA + EGCG by the CCK-8 assay. **(C)** Real-time PCR of changes in mRNA levels of TNFSF10 , MAPK1 and BID in PIG1. Data were presented as mean ± SEM of three independent experiments; **$P < 0.01$ compared with the control group; ##$P < 0.01$ compared with the 3-MA group.

Funding

Data availability statement

The data that support the findings of this study are openly available in the Gene Expression Omnibus database at http://www.ncbi.nlm.nih.gov/geo, the Human Autophagy Database at http://www.autophagy.lu/index.html and the Human Autophagy Database at http://www.autophagy.lu/index.html. The PCR data used to support the findings of this study are available from the corresponding author upon request.

CRediT authorship contribution statement

Wenwen Wang: Writing – original draft, Methodology, Formal analysis, Data curation. **Danfeng Xu:** Writing – original draft, Formal analysis, Data curation. **Youming Huang:** Validation, Data curation. **Xiaohua Tao:** Resources, Project administration. **Yibin Fan:** Resources, Project administration. **Zhiming Li:** Writing – review & editing, Supervision, Funding acquisition, Conceptualization. **Xiaoxia Ding:** Writing – review & editing, Validation, Methodology, Conceptualization.

Declaration of competing interest

The authors declare that they have no known competing financial interests or personal relationships that could have appeared to influence the work reported in this paper.

Appendix A. Supplementary data

Supplementary data to this article can be found online at https://doi.org/10.1016/j.heliyon.2023.e23220.

References

[1] C. Bergqvist, K. Ezzedine, Vitiligo: a review, Dermatology 236 (2020) 571–592, https://doi.org/10.1159/000506103.
[2] Y. Feng, Y. Lu, Advances in vitiligo: update on therapeutic targets, Front. Immunol. 13 (2022), 986918, https://doi.org/10.3389/fimmu.2022.986918.
[3] K. Ezzedine, A.M. Soliman, C. Li, H.S. Camp, A.G. Pandya, Comorbidity burden among patients with vitiligo in the United States: a large-scale retrospective claims database analysis, Dermatol. Ther. 13 (2023) 2265–2277, https://doi.org/10.1007/s13555-023-01001-2.
[4] A. De, N. Choudhary, A. Sil, A. Sarda, A.H. Hasanoor Raja, A cross-sectional study of the levels of cytokines IL-6, TNF-α, and IFN-γ in blood and skin (lesional and uninvolved) of vitiligo patients and their possible role as biomarkers, Indian J. Dermatol. 68 (2023) 67–72, https://doi.org/10.4103/ijd.ijd_27_22.
[5] V. Deretic, Autophagy in inflammation, infection, and immunometabolism, Immunity 54 (2021) 437–453, https://doi.org/10.1016/j.immuni.2021.01.018.
[6] J.N.S. Vargas, M. Hamasaki, T. Kawabata, R.J. Youle, T. Yoshimori, The mechanisms and roles of selective autophagy in mammals, Nat. Rev. Mol. Cell Biol. 24 (2023) 167–185, https://doi.org/10.1038/s41580-022-00542-2.
[7] M. Sorice, Crosstalk of autophagy and apoptosis, Cells 11 (2022) 1479, https://doi.org/10.3390/cells11091479.
[8] K. Prerna, V.K. Dubey, Beclin1-mediated interplay between autophagy and apoptosis: new understanding, Int. J. Biol. Macromol. 204 (2022) 258–273, https://doi.org/10.1016/j.ijbiomac.2022.02.005.
[9] L. Raam, E. Kaleviste, M. Šunina, H. Vaher, M. Saare, E. Prans, M. Pihlap, K. Abram, M. Karelson, P. Peterson, A. Rebane, K. Kisand, K. Kingo, Lymphoid stress surveillance response contributes to vitiligo pathogenesis, Front. Immunol. 9 (2018) 2707, https://doi.org/10.3389/fimmu.2018.02707.
[10] Y. He, S. Li, W. Zhang, W. Dai, T. Cui, G. Wang, T. Gao, C. Li, Dysregulated autophagy increased melanocyte sensitivity to H2O2-induced oxidative stress in vitiligo, Sci. Rep. 7 (2017), 42394, https://doi.org/10.1038/srep42394.
[11] E. Bastonini, D. Kovacs, S. Raffa, M. delle Macchie, A. Pacifico, P. Iacovelli, M.R. Torrisi, M. Picardo, A protective role for autophagy in vitiligo, Cell Death Dis. 12 (2021) 318, https://doi.org/10.1038/s41419-021-03592-0.
[12] Z. Su, H. Fang, H. Hong, L. Shi, W. Zhang, W. Zhang, Y. Zhang, Z. Dong, L.J. Lancashire, M. Bessarabova, X. Yang, B. Ning, B. Gong, J. Meehan, J. Xu, W. Ge, R. Perkins, M. Fischer, W. Tong, An investigation of biomarkers derived from legacy microarray data for their utility in the RNA-seq era, Genome Biol. 15 (2014) 3273, https://doi.org/10.1186/s13059-014-0523-y.
[13] Z. Lei, S. Yu, Y. Ding, J. Liang, Y. Halifu, F. Xiang, D. Zhang, H. Wang, W. Hu, T. Li, Y. Wang, X. Zou, K. Zhang, X. Kang, Identification of key genes and pathways involved in vitiligo development based on integrated analysis, Medicine (Baltim.) 99 (2020), e21297, https://doi.org/10.1097/MD.0000000000021297.
[14] A. Singh, V. Gotherwal, P. Junni, V. Vijayan, M. Tiwari, P. Ganju, A. Kumar, P. Sharma, T. Fatima, A. Gupta, A. Holla, H.K. Kar, S. Khanna, L. Thukral, G. Malik, K. Natarajan, C.J. Gadgil, R. Lahesmaa, V.T. Natarajan, R. Rani, R.S. Gokhale, Mapping architectural and transcriptional alterations in non-lesional and lesional epidermis in vitiligo, Sci. Rep. 7 (2017) 9860, https://doi.org/10.1038/s41598-017-10253-w.
[15] D. Toro-Domínguez, J. Martorell-Marugán, R. López-Domínguez, A. García-Moreno, V. González-Rumayor, M.E. Alarcón-Riquelme, P. Carmona-Sáez, ImaGEO: integrative gene expression meta-analysis from GEO database, Bioinformatics 35 (2019) 880–882, https://doi.org/10.1093/bioinformatics/bty721.
[16] E. Clough, T. Barrett, The gene expression Omnibus database, Methods Mol. Biol. 1418 (2016) 93–110, https://doi.org/10.1007/978-1-4939-3578-9_5.
[17] Y. Wang, W. Zhao, Z. Xiao, G. Guan, X. Liu, M. Zhuang, A risk signature with four autophagy-related genes for predicting survival of glioblastoma multiforme, J. Cell Mol. Med. 24 (2020) 3807, https://doi.org/10.1111/jcmm.14938.
[18] M. Ren, C.-Y. Wei, L. Wang, X.-Y. Deng, N.-H. Lu, J.-Y. Gu, Integration of individual prediction index based on autophagy-related genes and clinical phenomes in melanoma patients, Clin. Transl. Med. 10 (2020) e132, https://doi.org/10.1002/ctm2.132.
[19] K. Zhang, G. Shang, A. Padavannil, J. Wang, R. Sakthivel, X. Chen, M. Kim, M.G. Thompson, A. García-Sastre, K.W. Lynch, Z.J. Chen, Y.M. Chook, B.M. A. Fontoura, Structural–functional interactions of NS1-BP protein with the splicing and mRNA export machineries for viral and host gene expression, Proc. Natl. Acad. Sci. U. S. A. 115 (2018), E12218–E12227, https://doi.org/10.1073/pnas.1818012115.
[20] S. Bhattacharya, P. Dunn, C.G. Thomas, B. Smith, H. Schaefer, J. Chen, Z. Hu, K.A. Zalocusky, R.D. Shankar, S.S. Shen-Orr, E. Thomson, J. Wiser, A.J. Butte, ImmPort, toward repurposing of open access immunological assay data for translational and clinical research, Sci. Data 5 (2018), 180015, https://doi.org/10.1038/sdata.2018.15.
[21] M.E. Ritchie, B. Phipson, D. Wu, Y. Hu, C.W. Law, W. Shi, G.K. Smyth, Limma powers differential expression analyses for RNA-sequencing and microarray studies, Nucleic Acids Res. 43 (2015) e47, https://doi.org/10.1093/nar/gkv007.
[22] N. Zamaninour, A. Pazouki, M. Kermansaravi, A. Seifollahi, A. Kabir, Changes in body composition and biochemical parameters following laparoscopic one anastomosis gastric bypass: 1-year follow-up, Obes. Surg. 31 (2021) 232–238, https://doi.org/10.1007/s11695-020-04901-w.
[23] T. Wu, E. Hu, S. Xu, M. Chen, P. Guo, Z. Dai, T. Feng, L. Zhou, W. Tang, L. Zhan, X. Fu, S. Liu, X. Bo, G. Yu, clusterProfiler 4.0: a universal enrichment tool for interpreting omics data, Innovation 2 (2021), 100141, https://doi.org/10.1016/j.xinn.2021.100141.
[24] G. Yu, L.-G. Wang, Y. Han, Q.-Y. He, clusterProfiler: an R Package for comparing biological themes among gene clusters, OMICS 16 (2012) 284–287, https://doi.org/10.1089/omi.2011.0118.
[25] S.A. Aleksander, J. Balhoff, S. Carbon, J.M. Cherry, H.J. Drabkin, D. Ebert, M. Feuermann, P. Gaudet, N.L. Harris, D.P. Hill, R. Lee, H. Mi, S. Moxon, C. J. Mungall, A. Muruganugan, T. Mushayahama, P.W. Sternberg, P.D. Thomas, K. Van Auken, J. Ramsey, D.A. Siegele, R.L. Chisholm, P. Fey, M.C. Aspromonte, M.V. Nugnes, F. Quaglia, S. Tosatto, M. Giglio, S. Nadendla, G. Antonazzo, H. Attrill, G. dos Santos, S. Marygold, V. Strelets, C.J. Tabone, J. Thurmond, P. Zhou, S.H. Ahmed, P. Asanitthong, D. Luna Buitrago, M.N. Erdol, M.C. Gage, M. Ali Kadhum, K.Y.C. Li, M. Long, A. Michalak, A. Pesala, A. Pritazahra, S.C. C. Saverimuttu, R. Su, K.E. Thurlow, R.C. Lovering, C. Logie, S. Oliferenko, J. Blake, K. Christie, L. Corbani, M.E. Dolan, H.J. Drabkin, D.P. Hill, L. Ni, D. Sitnikov, C. Smith, A. Cuzick, J. Seager, L. Cooper, J. Elser, P. Jaiswal, P. Gupta, P. Jaiswal, S. Naithani, M. Lera-Ramirez, K. Rutherford, V. Wood, J.L. De Pons, M.R. Dwinell, G.T. Hayman, M.L. Kaldunski, A.E. Kwitek, S.J.F. Lauderkind, M.A. Tutaj, M. Vedi, S.-J. Wang, P. D'Eustachio, L. Aimo, K. Axelsen, A. Bridge, N. Hyka-Nouspikel, A. Morgat, S.A. Aleksander, J.M. Cherry, S.R. Engel, K. Karra, S.R. Miyasato, R.S. Nash, M.S. Skrzypek, S. Weng, E.D. Wong, E. Bakker, T.Z. Berardini, L. Reiser, A. Auchincloss, K. Axelsen, G. Argoud-Puy, M.-C. Blatter, E. Boutet, L. Breuza, A. Bridge, C. Casals-Casas, E. Coudert, A. Estreicher, M. Livia Famiglietti, M. Feuermann, A. Gos, N. Gruaz-Gumowski, C. Hulo, N. Hyka-Nouspikel, F. Jungo, P. Le Mercier, D. Lieberherr, P. Masson, A. Morgat, I. Pedruzzi, S. Pourcel, S. Poux, C. Rivoire, S. Sundaram, A. Bateman, E. Bowler-Barnett, H. Bye-A-Jee, P. Denny, A. Ignatchenko, R. Ishtiaq, A. Lock, Y. Lussi, M. Magrane, M.J. Martin, S. Orchard, P. Raposo, E. Speretta, N. Tyagi, K. Warner, R. Zaru, A.D. Diehl, R. Lee, J. Chan, S. Diamantakis, D. Raciti,

M. Zarowiecki, M. Fisher, C. James-Zorn, V. Ponferrada, A. Zorn, S. Ramachandran, L. Ruzicka, M. Westerfield, The gene Ontology knowledgebase in 2023, Genetics 224 (2023), https://doi.org/10.1093/genetics/iyad031 iyad031.

[26] The gene Ontology resource: 20 years and still GOing strong, Nucleic Acids Res. 47 (2019) D330–D338, https://doi.org/10.1093/nar/gky1055.

[27] W. Luo, M.S. Friedman, K. Shedden, K.D. Hankenson, P.J. Woolf, GAGE: generally applicable gene set enrichment for pathway analysis, BMC Bioinf. 10 (2009) 161, https://doi.org/10.1186/1471-2105-10-161.

[28] M. Kanehisa, M. Furumichi, Y. Sato, M. Kawashima, M. Ishiguro-Watanabe, KEGG for taxonomy-based analysis of pathways and genomes, Nucleic Acids Res. 51 (2022) D587–D592, https://doi.org/10.1093/nar/gkac963.

[29] M. Kanehisa, M. Furumichi, M. Tanabe, Y. Sato, K. Morishima, KEGG: new perspectives on genomes, pathways, diseases and drugs, Nucleic Acids Res. 45 (2017) D353–D361, https://doi.org/10.1093/nar/gkw1092.

[30] D. Szklarczyk, A.L. Gable, D. Lyon, A. Junge, S. Wyder, J. Huerta-Cepas, M. Simonovic, N.T. Doncheva, J.H. Morris, P. Bork, L.J. Jensen, C. von Mering, STRING v11: protein-protein association networks with increased coverage, supporting functional discovery in genome-wide experimental datasets, Nucleic Acids Res. 47 (2019) D607–D613, https://doi.org/10.1093/nar/gky1131.

[31] D. Szklarczyk, R. Kirsch, M. Koutrouli, K. Nastou, F. Mehryary, R. Hachilif, A.L. Gable, T. Fang, N.T. Doncheva, S. Pyysalo, P. Bork, L.J. Jensen, C. von Mering, The STRING database in 2023: protein–protein association networks and functional enrichment analyses for any sequenced genome of interest, Nucleic Acids Res. 51 (2022) D638–D646, https://doi.org/10.1093/nar/gkac1000.

[32] C.-H. Chin, S.-H. Chen, H.-H. Wu, C.-W. Ho, M.-T. Ko, C.-Y. Lin, cytoHubba: identifying hub objects and sub-networks from complex interactome, BMC Syst. Biol. 8 (2014) S11, https://doi.org/10.1186/1752-0509-8-S4-S11.

[33] H. Ma, Z. He, J. Chen, X. Zhang, P. Song, Identifying of biomarkers associated with gastric cancer based on 11 topological analysis methods of CytoHubba, Sci. Rep. 11 (2021) 1–11, https://doi.org/10.1038/s41598-020-79235-9.

[34] M. Franz, H. Rodriguez, C. Lopes, K. Zuberi, J. Montojo, G.D. Bader, Q. Morris, GeneMANIA update 2018, Nucleic Acids Res. 46 (2018) W60–W64, https://doi.org/10.1093/nar/gky311.

[35] D. Warde-Farley, S.L. Donaldson, O. Comes, K. Zuberi, R. Badrawi, P. Chao, M. Franz, C. Grouios, F. Kazi, C.T. Lopes, A. Maitland, S. Mostafavi, J. Montojo, Q. Shao, G. Wright, G.D. Bader, Q. Morris, The GeneMANIA prediction server: biological network integration for gene prioritization and predicting gene function, Nucleic Acids Res. 38 (2010) W214, https://doi.org/10.1093/nar/gkq537.

[36] A. Kikuchi, T. Soshi, T. Kono, M. Koyama, C. Fujii, Validity of short-term assessment of risk and treatability in the Japanese forensic probation service, Front. Psychiatr. 12 (2021), 645927, https://doi.org/10.3389/fpsyt.2021.645927.

[37] Y. Chen, X. Wang, miRDB: an online database for prediction of functional microRNA targets, Nucleic Acids Res. 48 (2020) D127–D131, https://doi.org/10.1093/nar/gkz757.

[38] V. Agarwal, G.W. Bell, J.-W. Nam, D.P. Bartel, Predicting effective microRNA target sites in mammalian mRNAs, Elife 4 (2015), https://doi.org/10.7554/eLife.05005.

[39] H.-Y. Huang, Y.-C.-D. Lin, J. Li, K.-Y. Huang, S. Shrestha, H.-C. Hong, Y. Tang, Y.-G. Chen, C.-N. Jin, Y. Yu, J.-T. Xu, Y.-M. Li, X.-X. Cai, Z.-Y. Zhou, X.-H. Chen, Y.-Y. Pei, L. Hu, J.-J. Su, S.-D. Cui, F. Wang, Y.-Y. Xie, S.-Y. Ding, M.-F. Luo, C.-H. Chou, N.-W. Chang, K.-W. Chen, Y.-H. Cheng, X.-H. Wan, W.-L. Hsu, T.-Y. Lee, F.-X. Wei, H.-D. Huang, miRTarBase 2020: updates to the experimentally validated microRNA–target interaction database, Nucleic Acids Res. 48 (2020) D148–D154, https://doi.org/10.1093/nar/gkz896.

[40] J.-H. Li, S. Liu, H. Zhou, L.-H. Qu, J.-H. Yang, starBase v2.0: decoding miRNA-ceRNA, miRNA-ncRNA and protein-RNA interaction networks from large-scale CLIP-Seq data, Nucleic Acids Res. 42 (2014) D92–D97, https://doi.org/10.1093/nar/gkt1248.

[41] D. Karagkouni, M.D. Paraskevopoulou, S. Chatzopoulos, I.S. Vlachos, S. Tastsoglou, I. Kanellos, D. Papadimitriou, I. Kavakiotis, S. Maniou, G. Skoufos, T. Vergoulis, T. Dalamagas, A.G. Hatzigeorgiou, DIANA-TarBase v8: a decade-long collection of experimentally supported miRNA–gene interactions, Nucleic Acids Res. 46 (2018) D239–D245, https://doi.org/10.1093/nar/gkx1141.

[42] C. Backes, Q.T. Khaleeq, E. Meese, A. Keller, miEAA: microRNA enrichment analysis and annotation, Nucleic Acids Res. 44 (2016) W110–W116, https://doi.org/10.1093/nar/gkw345.

[43] S. Fang, L. Dong, L. Liu, J. Guo, L. Zhao, J. Zhang, D. Bu, X. Liu, P. Huo, W. Cao, Q. Dong, J. Wu, X. Zeng, Y. Wu, Y. Zhao, HERB: a high-throughput experiment- and reference-guided database of traditional Chinese medicine, Nucleic Acids Res. 49 (2020) D1197–D1206, https://doi.org/10.1093/nar/gkaa1063.

[44] M. Holczer, B. Besze, V. Zámbó, M. Csala, G. Bánhegyi, O. Kapuy, Epigallocatechin-3-Gallate (EGCG) promotes autophagy-dependent survival via influencing the balance of mTOR-AMPK pathways upon endoplasmic reticulum stress, Oxid. Med. Cell. Longev. 2018 (2018), e6721530, https://doi.org/10.1155/2018/6721530.

[45] W. Ning, S. Wang, X. Dong, D. Liu, L. Fu, R. Jin, A. Xu, Epigallocatechin-3-gallate (EGCG) suppresses the trafficking of lymphocytes to epidermal melanocytes via inhibition of JAK2: its implication for vitiligo treatment, Biol. Pharm. Bull. 38 (2015) 1700–1706, https://doi.org/10.1248/bpb.b15-00331.

[46] X. Yi, W. Guo, Q. Shi, Y. Yang, W. Zhang, X. Chen, P. Kang, J. Chen, T. Cui, J. Ma, H. Wang, S. Guo, Y. Chang, L. Liu, Z. Jian, L. Wang, Q. Xiao, S. Li, T. Gao, C. Li, SIRT3-Dependent mitochondrial dynamics remodeling contributes to oxidative stress-induced melanocyte degeneration in vitiligo, Theranostics 9 (2019) 1614–1633, https://doi.org/10.7150/thno.30398.

[47] K.J. Gellatly, J.P. Strassner, K. Essien, M.A. Refat, R.L. Murphy, A. Coffin-Schmitt, A.G. Pandya, A. Tovar-Garza, M.L. Frisoli, X. Fan, X. Ding, E.E. Kim, Z. Abbas, P. McDonel, M. Garber, J.E. Harris, scRNA-seq of human vitiligo reveals complex networks of subclinical immune activation and a role for CCR5 in Treg function, Sci. Transl. Med. 13 (2021), eabd8995, https://doi.org/10.1126/scitranslmed.abd8995.

[48] Y. Xuan, Y. Yang, L. Xiang, C. Zhang, The role of oxidative stress in the pathogenesis of vitiligo: a culprit for melanocyte death, Oxid. Med. Cell. Longev. 2022 (2022), 8498472, https://doi.org/10.1155/2022/8498472.

[49] D.J. Klionsky, G. Petroni, R.K. Amaravadi, E.H. Baehrecke, A. Ballabio, P. Boya, J.M.B.-S. Pedro, K. Cadwell, F. Cecconi, A.M.K. Choi, M.E. Choi, C.T. Chu, P. Codogno, M.I. Colombo, A.M. Cuervo, V. Deretic, I. Dikic, Z. Elazar, E.-L. Eskelinen, G.M. Fimia, D.A. Gewirtz, D.R. Green, M. Hansen, M. Jäättelä, T. Johansen, G. Juhász, V. Karantza, C. Kraft, G. Kroemer, N.T. Ktistakis, S. Kumar, C. Lopez-Otin, K.F. Macleod, F. Madeo, J. Martinez, A. Meléndez, N. Mizushima, C. Münz, J.M. Penninger, R.M. Perera, M. Piacentini, F. Reggiori, D.C. Rubinsztein, K.M. Ryan, J. Sadoshima, L. Santambrogio, L. Scorrano, H.-U. Simon, A.K. Simon, A. Simonsen, A. Stolz, N. Tavernarakis, S.A. Tooze, T. Yoshimori, J. Yuan, Z. Yue, Q. Zhong, L. Galluzzi, F. Pietrocola, Autophagy in major human diseases, EMBO J. 40 (2021), https://doi.org/10.15252/embj.2021108863.

[50] L. Ma, Z. Wang, M. Xie, Y. Quan, W. Zhu, F. Yang, C. Zhao, Y. Fan, N. Fang, H. Jiang, Q. Wang, S. Wang, J. Zhou, X. Chen, Y. Shu, Silencing of circRACGAP1 sensitizes gastric cancer cells to apatinib via modulating autophagy by targeting miR-3657 and ATG7, Cell Death Dis. 11 (2020) 169, https://doi.org/10.1038/s41419-020-2352-0.

[51] Y. Wang, C. Xia, L. Chen, Y.C. Chen, Y. Tu, Saponins extracted from tea (camellia sinensis) flowers induces autophagy in ovarian cancer cells, Molecules 25 (2020) 5254, https://doi.org/10.3390/molecules25225254.

[52] C. He, G. Liu, S. Zhuang, J. Zhang, Y. Chen, H. Li, Z. Huang, Y. Zheng, Yu nu compound regulates autophagy and apoptosis through mTOR in vivo and vitro, Diabetes Metab Syndr Obes 13 (2020) 2081–2092, https://doi.org/10.2147/DMSO.S253494.

[53] K.-Y. Kim, K.-I. Park, S.-H. Kim, S.-N. Yu, S.-G. Park, Y.W. Kim, Y.-K. Seo, J.-Y. Ma, S.-C. Ahn, Inhibition of autophagy promotes salinomycin-induced apoptosis via reactive oxygen species-mediated PI3K/AKT/mTOR and ERK/p38 MAPK-dependent signaling in human prostate cancer cells, Int. J. Mol. Sci. 18 (2017) 1088, https://doi.org/10.3390/ijms18051088.

[54] D. Sag, Z.O. Ayyildiz, S. Gunalp, G. Wingender, The role of TRAIL/DRs in the modulation of immune cells and responses, Cancers 11 (2019) 1469, https://doi.org/10.3390/cancers11101469.

[55] J. Cao, Y. Zhang, Y. Chen, S. Liang, D. Liu, W. Fan, Y. Xu, H. Liu, Z. Zhou, X. Liu, S. Hou, Dynamic transcriptome reveals the mechanism of liver injury caused by DHAV-3 infection in pekin duck, Front. Immunol. 11 (2020), 568565, https://doi.org/10.3389/fimmu.2020.568565.

[56] A. Mohr, T. Chu, G.N. Brooke, R.M. Zwacka, MSC.sTRAIL has better efficacy than MSC.FL-TRAIL and in combination with AKTi blocks pro-metastatic cytokine production in prostate cancer cells, Cancers 11 (2019) 568, https://doi.org/10.3390/cancers11040568.

[57] V. Kedinger, S. Muller, H. Gronemeyer, Targeted expression of tumor necrosis factor-related apoptosis-inducing ligand TRAIL in skin protects mice against chemical carcinogenesis, Mol. Cancer 10 (2011) 34, https://doi.org/10.1186/1476-4598-10-34.

[58] P. O'Reilly, C. Ortutay, G. Gernon, E. O'Connell, C. Seoighe, S. Boyce, L. Serrano, E. Szegezdi, Co-acting gene networks predict TRAIL responsiveness of tumour cells with high accuracy, BMC Genom. 15 (2014) 1144, https://doi.org/10.1186/1471-2164-15-1144.

[59] L. Xue, W. Zhang, Y. Ju, X. Xu, H. Bo, X. Zhong, Z. Hu, C. Zheng, B. Fang, S. Tang, TNFSF10, an autophagy related gene, was a prognostic and immune infiltration marker in skin cutaneous melanoma, J. Cancer 14 (2023) 2417–2430, https://doi.org/10.7150/jca.86735.

[60] W. He, Q. Wang, J. Xu, X. Xu, M.T. Padilla, G. Ren, X. Gou, Y. Lin, Attenuation of TNFSF10/TRAIL-induced apoptosis by an autophagic survival pathway involving TRAF2- and RIPK1/RIP1-mediated MAPK8/JNK activation, Autophagy 8 (2012) 1811, https://doi.org/10.4161/auto.22145.

[61] Y. Li, J. Huang, J. Lu, Y. Ding, L. Jiang, S. Hu, J. Chen, Q. Zeng, The role and mechanism of Asian medicinal plants in treating skin pigmentary disorders, J. Ethnopharmacol. 245 (2019), 112173, https://doi.org/10.1016/j.jep.2019.112173.